Hydro-Abrasive Jet Machining Modeling for Computer Control and Optimization

R. Groppetti and F. Jovane

Use of hydro-abrasive jet machining (HAJM) for machining a wide variety of materials—metals, polymers, ceramics, fiber-reinforced composites, metal-matrix composites, and bonded or hybridized materials—primarily for two- and three-dimensional cutting and also for drilling, turning, milling, and deburring, has been reported. However, the potential of this innovative process has not been explored fully. This article discusses process control, integration, and optimization of HAJM to establish a platform for the implementation of real-time adaptive control constraint (ACC), adaptive control optimization (ACO), and CAD/CAM integration. It presents the approach followed and the main results obtained during the development, implementation, automation, and integration of a HAJM cell and its computerized controller. After a critical analysis of the process variables and models reported in the literature to identify process variables and to define a process model suitable for HAJM real-time control and optimization, to correlate process variables and parameters with machining results, and to avoid expensive and time-consuming experiments for determination of the optimal machining conditions, a process prediction and optimization model was identified and implemented. Then, the configuration of the HAJM cell, architecture, and multiprogramming operation of the controller in terms of monitoring, control, process result prediction, and process condition optimization were analyzed. This prediction and optimization model for selection of optimal machining conditions using multi-objective programming was analyzed. Based on the definition of an economy function and a productivity function, with suitable constraints relevant to required machining quality, required kerfing depth, and available resources, the model was applied to test cases based on experimental results.

Keywords

ACC, adaptive control, CAD/CAM, hydro-abrasive jet machining, multi-objective optimization

1. Introduction

HYDRO-ABRASIVE jet machining has been used for machining a wide variety of materials (metals, polymers, ceramics, fiber-reinforced composites, metal-matrix composites, and bonded or hybridized materials, etc.) primarily for two-dimensional cutting operations, but also for three-dimensional cutting operations and for drilling, turning, milling, and deburring.[1-5] This process is based on use of a high-speed jet formed by a stream of abrasive particles that are focused, mixed, and accelerated by a high-speed hypersonic jet of water, from a nozzle under pressures of up to 400 MPa. The hydro-abrasive jet impinges on a localized area of the workpiece, causing complex micromachining interactions with the material, such as erosion, abrasion, cavitation, and brittle fracture. The HAJM process has many advantages, including flexibility of application due to omnidirectional noncontact cutting, changes in contour, shape, and angle, as well as changes in process parameters, variables, and cutting patterns. Moreover, many advantages are relevant to the quality of the workpiece when the HAJM material removal process is used, in terms of negligible thermal, structural, and mechanical damage such as strain hardening in metals and delamination in composites, a clean, precise workpiece edge, with limited burr formation, depending on material properties and process condition. Therefore, research and industrial efforts have been devoted to the study of HAJM to fully exploit the potential of this process in terms of productivity, quality, flexibility, economy, automation, and integration into the manufacturing process.[6-11] The HAJM process offers several benefits when used in the machining operations, such as (1) minimal workpiece material loss and material savings due to reduced kerf and closer parts spacing, and minimal environmental pollution, because the hydro-abrasive jet controls dust in atmospheric conditions and machining also can be performed under water; (2) a high cutting feed rate that can be controlled to achieve optimal cutting conditions; (3) easy control of process parameters, such as water pressure and jet energy, abrasive mass flow rate, feed rate, and standoff distance; and (4) the ability to cut any material.

The HAJM process is used for two- and three-dimensional cutting and for drilling[4,12] turning,[2] milling,[2,5] deburring,[1] and more generally for machining processes.[5,13,14] Computerized controllers are well suited for HAJM process control, particularly in two- and three-dimensional applications, where it is possible to control any path by maintaining a suitable, generally constant standoff distance to achieve the desired machining results.

To study and demonstrate the great potential of this innovative process, the authors have developed a hierarchical control architecture for the automation, integration, and optimization of the HAJM process and a specific method to study real-time adaptive control constraint (ACC), adaptive control optimization (ACO),[15] and CAD/CAM integration. They have also implemented a HAJM integrated computer-controlled cell. This article presents the approach followed and the main results obtained during the development and implementation of a

R. Groppetti, Università degli studi di Perugia, Italy; and **F. Jovane,** Politecnico di Milano, Italy.

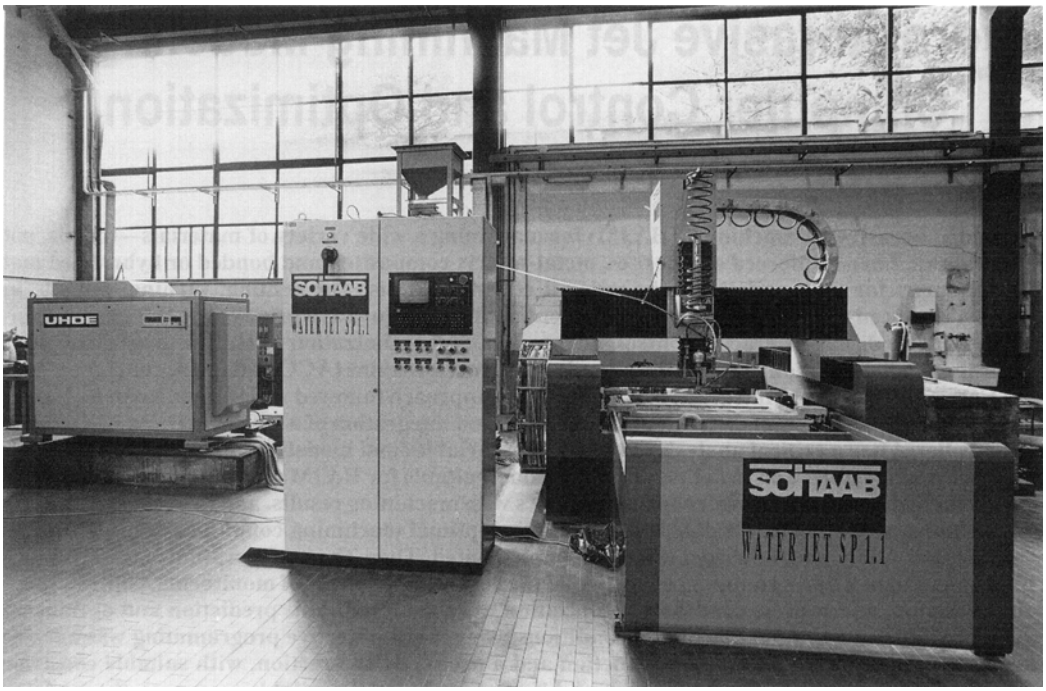

Fig. 1 HAJM cell setup.

HAJM cell and its computerized controller. A critical analysis of the process variables and models available in the literature is presented, to identify process variables and to define a process model suitable for HAJM real-time control and optimization. In addition to HAJM process control, in an attempt to correlate process variables and parameters with machining results, both a process model and an optimization model are necessary to avoid expensive and time-consuming experiments to determine optimal machining conditions. The current work describes the configuration of the cell and the specific components used to facilitate complete computerized control of the process, as well as the setup of the controller, which can process several logical and analog signals from different modules of the cell to achieve multiprogramming, process monitoring, and facilitate control of process parameters through multi-objective optimization.

A prediction and optimization model is presented, which identifies optimal machining conditions using multi-objective programming. This model is based on the definition of an economy function and a productivity function, with suitable constraints relevant to required machining quality, required kerfing depth, and available resources. A test case based on experimental results is presented and discussed to validate the model.

This activity has been developed in cooperation with industrial companies, following a "from the bottom up" approach, covering material removal process analysis to the integration of several components and subsystems to achieve a holistic view of the HAJM process. The configuration of the cell and the specific components used must allow complete computerized control of the process, and the setup of the controller must be capable of managing several logical and analog signals from different modules of the cell to facilitate process monitoring, controlling, predetermination of process parameters, and optimization of process conditions. Also, it must be open to integrate these functions at a low and high level of control.[16]

Identification of process variables and parameters and definition of a process model suitable for HAJM real-time control and optimization, as well as a critical analysis of the models presented in the literature, were undertaken to avoid expensive and time-consuming experiments and tests to determine optimal machining conditions in the industrial practice and to correlate HAJM process variables and parameters with the subsequent machining results.

An optimization model and a technological module were studied to identify optimal machining conditions using multi-objective programming. This model, based on the definition of an economy function and a productivity function, with suitable constraint functions relevant to the desired machining quality and the available resources, was implemented in an optimization technological module that was validated by experimental results of machining operations.

2. HAJM Cell Architecture and Operation

A fully computer controlled HAJM cell has been studied and implemented for HAJM process control analysis, optimization, and integration (see Fig. 1). The approach followed for the flexible and integrated automation of the cell has been "from the bottom up," starting with HAJM process analysis and study of the specific components and subsystems designed

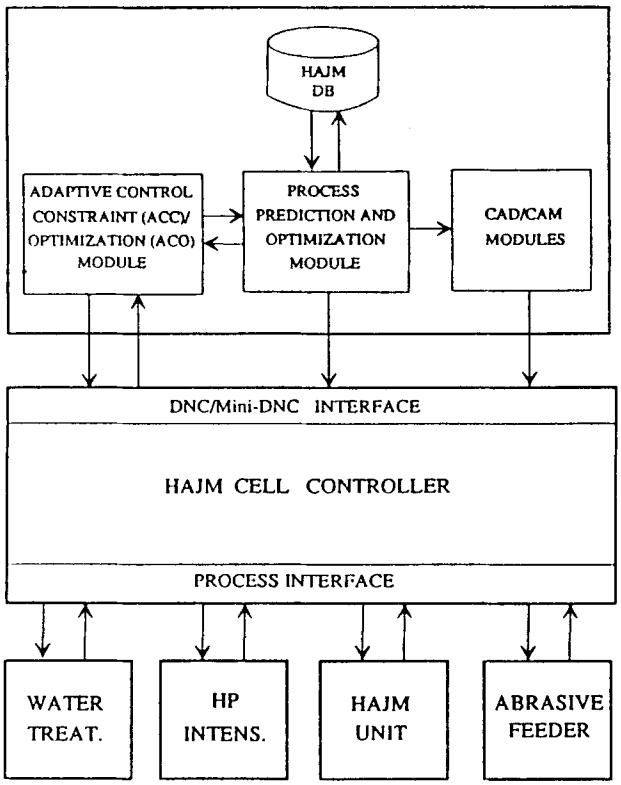

Fig. 2 Schematic of HAJM cell architecture.

for computer automation and integration, moving toward complete integration in a computerized environment.[16-18] The controller has been designed to control and integrate these components and subsystems within the cell. Therefore, a suitable interface with the process, a multiprocessing control architecture, integration capabilities, and a suitable user interface with graphics capabilities has been adopted to execute numerous real-time and off-line tasks.

2.1 *Physical Architecture*

The physical architecture of the HAJM cell is based on subsystems and modules controlled by a control hierarchy. An advanced high-pressure pump or intensifier, a reciprocating plunger pump, which is controlled by a dedicated controller to supply a constant, highly pressurized stream of water to manage the input/output signals to and from the cell controller and execute intensifier monitoring and diagnostics, supplies the high-pressure water to a nozzle valve that is pneumatically or electrically activated. A mixing chamber generates a consistent hydro-abrasive jet by means of jewel nozzle, or primary nozzle, and a focuser, or secondary nozzle.

A machining unit with a workpiece loading and unloading device, with three linear axes (X, Y, and Z) and two angular axes (A and B), is controlled by a computerized numerical controller (CNC) capable of executing input/output data to and from the field, as well as direct numerical control (DNC) and mini-DNC communication. The CNC also performs the tasks of cell controller, sequence monitoring, controlling and integrating subsystems and components of the cell, and communicating with a host computer with peripherals via DNC and mini-DNC for CAD/CAM integration. It also interfaces with a dedicated computer for process variables prediction and optimization and for adaptive control constraint (ACC) and adaptive control optimization (ACO) (Fig. 2).

Additionally, a reverse osmosis water treatment subsystem feeds low-pressure water to the intensifier; a high-pressure line supplies water to the nozzle. Then a catcher collects the exhaust jet after the cut and a separator filters abrasives and particles of material that has been removed.

2.2 *Control Architecture and Multiprogramming Operation*

The control architecture is based on an advanced CNC with a modular hardware and software expandable multiprocessor configuration, allowing multiprocessing operation and network integration in a control hierarchy[19] by means of machining unit axes motion control, cell status and sequence control, input/output signals to and from the field, and communication with the control hierarchy.

The hardware architecture of the controller is based on a multiprocessor minicomputer with system CPUs, axes manager CPUs, digital I/O CPUs, with memory, communication boards, operator panel interface, transducer boards, A/D-D/A converter boards, and I/O boards connected with a local and system bus. Therefore, the system architecture of the controller can be subdivided into two basic components: the first devoted to real-time processing and higher level integration, the second interfacing with the process and the cell.

The minicomputer is based on processors linked through a serial RS-422 line, with mathematical coprocessors and memory, and is capable of real-time control of the machining unit and of the cell, by means of a digital and analog integrated interface to the field, with a user interface and peripheral interface. The controller communication capabilities are based on point-to-point connection for file transfer by means of a mini-DNC communication protocol for CAD/CAM integration and of a peripheral communication system (PSC) for DNC integration, multidrop connection by means of Data Highway II (DHII), and remote digital I/O oriented.

From a software point of view, the controller software can be subdivided into (1) base software that is common to all the applications (operating system multitasking, time/event driven, service software, background partition, editing, file operations, diagnostics, machine logic interface development); (2) machining unit software that is specific to any machining unit (language and development systems, system interface programming, environment and facilities, diagnostics, debug and setup facilities, end user-oriented diagnostics, enhanced features for specific requirements by means of a custom software interface); (3) application software that is common to a specific process (ISO standard language and a geometrical and technological language (GTL) parts programming, Advanced Super Set Extension Tool (ASSET) for files handling, system variables, digital and analog input/output and serial lines, display and keyboard managing from parts program; and (4) a multiprogramming language that allows simultaneous activation and synchronization of additional parts programs, where the operator module can be common or shared.

The custom software interface (CSI) makes all of the computing resources of the controller available to the user and makes it possible for the designer and system integrator to access input/output memory mapped areas by means of assembler or high level languages, to develop dedicated and specific applications.

ASSET language facilitates use of high-level parts programming and handling and accessing of data files, system variables (such as axes positions, input/output digital and analog signals, and serial lines status), and peripherals (such as keyboard and monitor with graphics capabilities). Finally, controller-integrated software interface with the field can be programmed by the programmable interface system (SIPROM), which is a high-level language oriented toward logical signals handling and the characterization of the functionality and operation of the machining unit and the cell.

Three real-time processes have been implemented to provide control of the three axes and HAJM process control: real-time override of HAJM process variables; data acquisition and HAJM process parameter and variable real-time monitoring; and HAJM process parameter predetermination and optimal conditions estimation.

The systematic design and implementation of the cell controller has been carried out following a methodology that is based on the following:

- Objective definition
- Subsystem and component analysis
- Functional model and data analysis
- Data acquisition and processing resources requirements
- Hardware controller architecture
- Base software design, debug, and validation
- Application software design, debug, and validation
- System integration and validation

Machining unit characterization files and a cell/controller interface have been developed and implemented in a program executed with cycles relevant to the control system, unit, cell subsystems that activate the HAJM process variables, timing and sequences, axes movements, part loading and unloading, water treatment, and jet catcher.[19]

The methodology followed during the study, development, and implementation of the HAJM cell began with an analysis of the physical and logical components and subsystems of the HAJM process with the goal of automation and integration. To achieve control and optimization of the HAJM process, the following development steps were followed:

- Determine suitable process variables, parameters, and models for computer control and machining condition optimization
- Monitor important process variables by means of suitable sensors and data acquisition and processing procedures
- Determine machinable depth of cut or thickness by means of suitable process models and algorithm and computing resource allocation
- Process optimization by means of multi-objective programming
- Implement and validate the developed solutions based on test cases

A technological process prediction and optimization module has been developed and integrated into the hierarchical control architecture of the HAJM process cell. This module, integrated with a technological database for HAJM, predetermines optimal process parameters and variables, provided off-line to the CAD/CAM system, to plan and make available an optimized parts program, and to the adaptive control constraint (ACC) and adaptive control optimization (ACO) to operate in real-time, respectively, in constrained or in optimized conditions (Fig. 2). Monitoring of the HJM/HAJM process is done by sensors, such as high-pressure transducers, position transducers for axes and standoff distances, water flow rate and abrasive mass flow rate sensors, solid-state camera for kerf width and jet diameter measurement, cutting force sensors, etc. A monitoring process has been implemented in the controller both for HJM and HAJM, and the primary data are shown on the controller readout and made available to the upper level control hierarchy. The visualization combines actual variables, acquired from the field, with programmed and set variables and parameters.

Regarding the prediction of machinable depth of cut corresponding to the expected thickness of the workpiece, suitable models have been studied for HAJM and implemented in a technological process prediction and optimization module. Due to the available computing resources in the controller, these models have been expressed using suitable algorithms of numerical analysis that make possible evaluation of the depth of cut starting from the selected parameter of the process. An interactive and iterative procedure allows identification of a predicted depth of cut equal to the depth of cut to be machined, and the identification of the relevant process variables and parameters to be set. The predicted depth of cut and the associated parameters and variables can be visualized on the readout of the controller. A complete analysis of the prediction algorithms and of their implementation is reported in Ref 20. Experimental HAJM data also can be collected and stored in a technological data base.

Prediction of optimal machining conditions, in terms of optimized HAJM process variables and parameters, establishes a fundamental step for HAJM computer control and optimization. This is done to avoid expensive and time-consuming experiments and tests and to guarantee the required productivity, quality, and economy in production. A HAJM optimization model can establish the basis for the study and implementation of a real-time adaptive control optimization (ACO) module.[15,21] A HAJM process prediction and optimization module has been devised and implemented that is capable of evaluating HAJM optimized variables and parameters. The optimized data can be input into the controller directly by the operator with a manual data input (MDI) procedure, or input automatically through a DNC or Mini-DNC interface. Data also can be input into the CAD/CAM subsystem at the CAM module level to obtain an optimized parts program, or in the ACO module for further real-time processing. The ACO module can implement an on-line adaptive control (AC) optimum machining condition strategy, based on the results of the off-line optimization procedure. Finally, optimized data can be

Table 1 Classification of HJM and HAJM variables and parameters

Classes	Variables and parameters	Abbreviation
HJM/HAJM		
Hydraulics	Water pressure	P
	Primary nozzle diameter	d_n
	Primary nozzle shape	N_s
	Primary nozzle material	N_m
	Water flow rate (water pressure, nozzle diameter, nozzle efficiency)	m_w
	Polymer concentration in water (only HJM)	c
Machining	Feed rate	u
	Standoff distance	s
	Number of passes	N
	Cutting angle	α
HAJM		
Mixing chamber/focuser	Mixing chamber dimension and shape	M_s
	Focuser diameter	d_j
	Focuser length	L_j
	Focuser shape	F_s
	Focuser material	F_m
Abrasive	Density	ρ_p
	Hardness	H_d
	Particle size	G_r
	Particle radius	r_p
	Particle moment of inertia	I_p
	Particle roundness	R_f
	Mass flow rate	$\dot{m}$
	Feeding effect (pressure, Venturi effect)	F_e
	Condition (slurried, dried)	C_s

stored in the technological HAJM database for future applications.

3. HAJM Modeling for Control and Optimization

A critical analysis of HAJM models, presented in the literature, was carried out to identify and evaluate process variables and parameters and to define process models suitable for HAJM real-time monitoring, control, variables prediction, and optimization. At the same time, the analysis was extended to hydro jet machining (HJM), i.e., to the process that uses only pressurized water, no abrasives.

3.1 *HAJM Variables and Models*

Analysis of HAJM and HJM has been performed on a holistic approach, because even if specific variables are relevant to abrasive system, such as abrasive mass flow rate, mixing chamber and focuser nozzle, some common classes of variables that are relevant to hydraulic and material removal mechanisms can be considered and classified. Classification of the primary HAJM and HJM variables and parameters is presented in Table 1.[6-8,22,23] A complete analysis of the effect of HJM/HAJM variables on cutting geometry, economy, and quality of cutting conditions has been presented in Ref 8 and 22.

Also, a critical analysis of the HJM and HAJM models presented in the literature has been carried out. This analysis addressed the identification of the more recurrent variables and parameters and defined process models suitable for HAJM monitoring, control, prediction, and optimization. Also, a complete analysis of these models has been presented in Ref 8 and 22. Figure 3 summarizes this analysis.[22]

A theoretical model was presented in Ref 24 and 25 that uses a control volume analysis to determine the hydrodynamic forces acting on the solid boundaries of a cutting slot, and on a Bingham model,[26] used to describe the time-dependent stress-strain relationship of a variety of solid materials; this model is suitable for the study and implementation of an algorithm for HJM depth of cut predetermination in the technological process prediction and optimization module, in a closed form solution in the form of a nondimensional cutting equation obtained from the following:

$$h = d_n \left\{ \frac{1 - (\sigma_c / \rho V_1^2)}{2C_f / \pi} \left[1 - e^{-(2C_f/\pi)(\rho V_1 / \eta)(V_1/u)} \right] \right\} \quad [1]$$

where h is the depth of cut; d_n is the nozzle diameter; C_f is the friction coefficient; η is the damping coefficient; σ_c is the compressive yield strength; ρ is the water density; V_1 is the water jet velocity at the input of the cutting slot; and u is the feed rate. Other models have been analyzed extensively in Ref 8 and 22.

A model of the HAJM process has been presented in the literature,[2,27-29] based on the erosion and abrasion processes caused by the hydro-abrasive jet. The model uses existing theories on the erosion of metals by solid particle impact, while site erosion models are considered for the effect of hydrodynamic loading on engaged particles during cutting.

The material removal process was modeled after two interaction modes. The first is a cutting wear mechanism that occurs at the top of the kerf primarily due to particle impact at shallow angles. The second is a deformation wear mode that occurs deeper in the kerf and is due to large impact angles. A simplified global material removal model is proposed to predict the depth of cut as a function of HAJM process variables and parameters. For the two interaction modes, the depth of cut, h_c, due to cutting wear, and the depth of cut, h_d, due to deformation wear, can be evaluated using the following equations:

$$h_c = \frac{14cd_j}{2.5\pi} \frac{\dot{m}}{\rho_P u d_j^2} \frac{1}{[(14/\pi)(\dot{m}/\rho_P u d_j^2)(V_f/C_k)^{2.5}]^{3/5}} (V_f/C_k)^{2.5} \quad [2]$$

$$h_d = \frac{1}{\pi d_j \sigma u / \left[2C_l \dot{m} (V_i - V_c)^2 \right] + (C_f / d_j) V_i / (V_i - V_c)} \quad [3]$$

where d_j is the jet diameter at the output from the secondary nozzle or focuser; $\dot{m}$ is the abrasive mass flow rate; V_i is the actual water jet velocity; C_k is the characteristic velocity; C_l is the

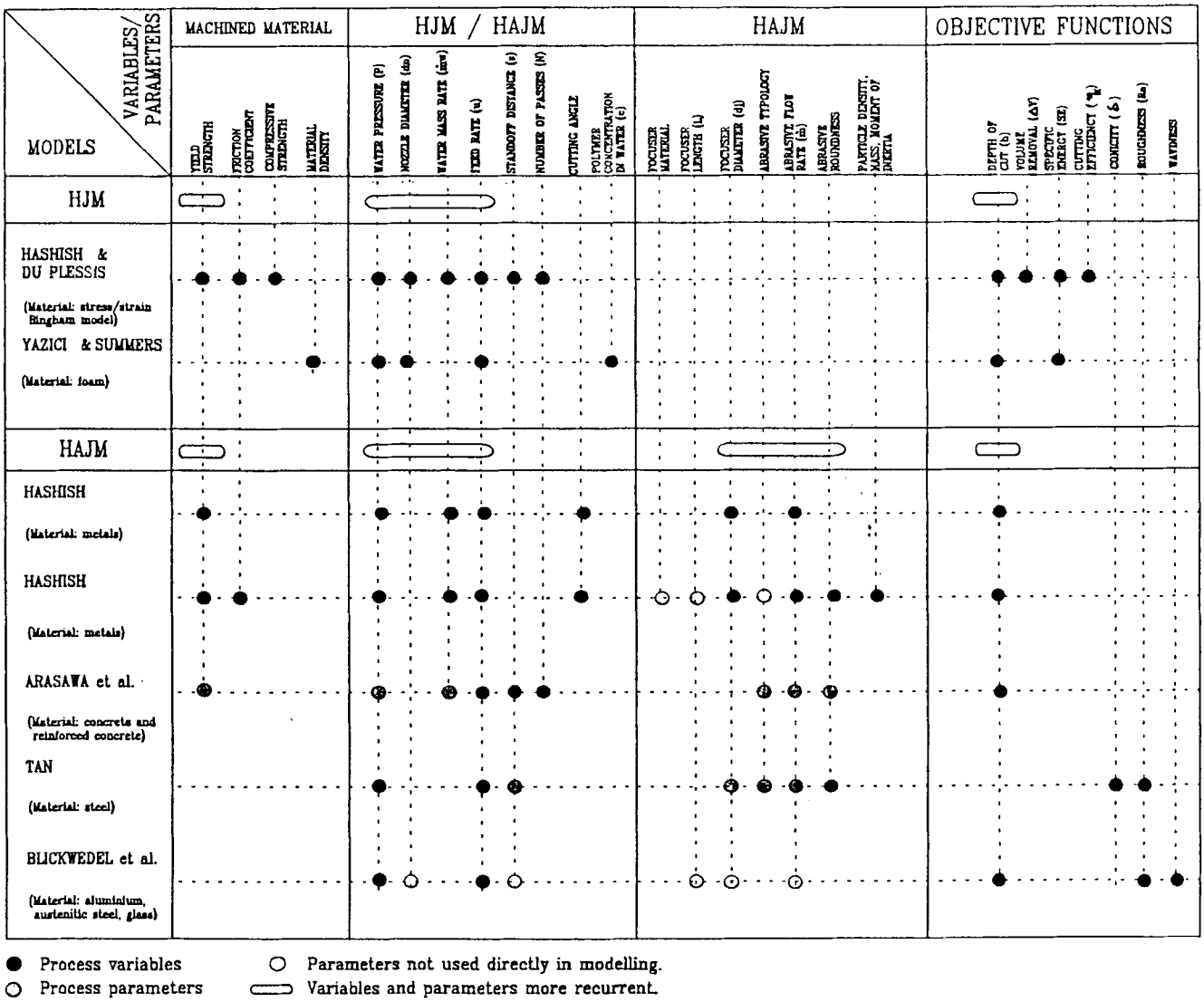

Fig. 3 Summary of HJM/HAJM models, variables and parameters, and objective functions.

impact efficiency of abrasive particles; ρ_P is the density of abrasive particle; u is the feed rate; c is the deformation/cutting wear parameters; σ is the material dynamic flow stress under the impingement of the jet; V_c is the threshold particle velocity; and C_f is the friction coefficient on the kerf wall. The global depth of cut h can be predicted by means of the following equation,[13] which is a linear combination of the previous equations:

$$h = d_j\{N_c[\text{Eq 2}] + N_d[\text{Eq 3}]\} \quad [4]$$

where N_c is the nondimensional number of depth of cut due to cutting wear, and N_d is the nondimensional number of depth of cut due to deformation wear. Also, for this model, a critical analysis is reported in Ref 8 and 22.

Eq 4 has been used in the technological process prediction and optimization module as a prediction model for the depth of penetration and as a cutting constraint in HAJM optimization multi-objective programming.

In addition to the previous models that take into account the prediction of HJM and HAJM depth of cut (i.e., an objective function related to process capability in terms of material removal), other models that take into account the quality of the workpiece machined by a hydro-abrasive jet were analyzed. The model proposed in Ref 30 takes into account the effect of HAJM variables and parameters, such as water supply pressure, jet feed rate, and abrasive particle size, on the kerf surface finish. The HAJM surface finish is characterized by striations; the model suggests that these striations are due to the kinematics/geometry of the cutting process rather than to any dynamics of the process such as jet instability. This approach does not require extensive knowledge of the physical micromachining mechanisms involved in the process, and it can be used to limit the empirical tests generally necessary to successfully apply HAJM. The model is based on an approach that does not differ-

entiate between the entry stage of the jet and a cyclic cutting stage, because the kinematics of the cutting process do not change during these two stages. The jet exit stage is associated with an outward deflection of the jet, thus producing an uncut portion.

Considering the energy dissipation during HAJM, a cycling mechanism is suggested to generate the striated surface finish. The model provides the rate of penetration of the material as the velocity of the tip of the jet. Therefore, the depth of cut, or greater penetration, h, is given by the equation:

$$h = h_m[1 - e^{-Bx_0/(\lambda/x_0)}] \quad [5]$$

where h_m is the maximum depth of penetration when the feed rate is almost zero; λ is the wavelength of the striation; x_0 is the point where jet diameter is equal to zero within a cycle; B is a parameter that depends on all of the HAJM parameters, such as water pressure, P, abrasive particle size, g, feed rate, u, nozzle diameter, d_j, standoff distance, X, etc.; it is assumed to be a constant.

Moreover, the model provides an expression of the cyclic change in jet diameter, D, producing the characteristic striations on the kerf surface, as follows:

$$D = D_o\left[1 - e^{-A[h_m - h)/h]^2(x_e - x_0)/\lambda - x_0)}\right] \quad [6]$$

where D_o can be considered the jet diameter at the input ($h - 0$) and is equal to the diameter d_j at the output from the nozzle; x_e is the displacement within each cycle; A is a function similar to B; and it is assumed to be expressed by the simplified relationship:

$$A = KPg/u^2 \quad [7]$$

where K is a conicity factor.

Assuming $x_e = \lambda$, the diameter, D_m, at the end of each cycle can be obtained from Eq 7 as the following:

$$D_m = D_o\left[1 - e^{-A[h_m - h)/h]^2}\right] \quad [8]$$

From this equation, a kerf conicity function δ

$$\delta = [D_o - D_m(h)]/h \quad [9]$$

has been obtained and applied within the technological process prediction and optimization module as quality constraint in the HAJM optimization multi-objective programming.

To summarize the critical analysis of the models, see Fig. 3 for a summary of HJM/HAJM models, variables, parameters, and objective functions.

3.2 *HAJM Multi-Objective Optimization*

To optimize the HAJM process, it is necessary to establish the preferred objective functions. From the critical analysis of the studies on HAJM and HJM reported in the literature, the typical objective functions that are generally used are shown in Fig. 3 and classified in Table 2. Some objective functions are identified and classified into three classes relevant to material removal rate (or productivity), machining quality, and machining economy.

Table 2 Classification of HAJM objective functions

Classes	Objective functions	Expression	Application field
Material removal rate (productivity)...	Depth of cut	h (see Eq 4)	Generic
	Removed thickness per unit-time	$\dot{h} = dh/dt$	Drilling
	Removed area per unit-time	$\dot{A} = hu$	Cutting
	Removed volume per unit-time	$\dot{V} = huw$	Milling
	Removed volume per unit-length	$\Delta V = hw$	Generic
	Cutting efficiency	$\eta_c = \Delta v/\left(0.5\dot{m}v_f^2\right)$	Generic
	Specific energy	$SE = (0.5\,\dot{m}V^2t)/\Delta V$	Mining
Machining quality level.....	Kerf width	w	Generic
	Conicity	δ	Generic
	Waviness	W_s	Generic
	Surface roughness	R_a	Generic
	Material damage	...	Generic
	Delamination	...	Composites
Machining economy.....	Cost per unit-machined length/unit-removed volume per unit-time	C (see Eq 16)	Generic

It is possible to identify several objective functions that can be expressed by means of suitable models. It is also possible to associate suitable quantitative expressions to some objective functions that usually have a qualitative meaning. Some objective functions have a generic applications field, whereas others have a specific application. The most important objective functions are a material removal rate or productivity objective function and a machining economy objective function, whereas the material removal quality can be considered a quality constraint to be satisfied as far as a delivery time constraint, or a constraint relevant to the available manufacturing resources, or a constraint relevant to a given application.

The objective functions listed in Table 2 generally are used in the literature as single-objective optimization models. An in-depth analysis of HAJM optimization has pointed out that a more suitable HAJM optimization model should be selected. In fact, single-objective programming optimization models do not capture the complexity of this problem. Moreover, because optimization models play a central role in the machining resources planning process, the type of model presents a significant effect on the planning stage and on the optimization results. Single-objective programming models require the use of a single measure of effectiveness, which encompasses data and parameters estimation and offers limited choices for the decisionmaker. Therefore, a suitable system analysis and planning procedure must be based on a multi-objective approach.[34]

The approach followed was based on a stepped planning methodology:

- Identification and quantification of objectives
- Definition of objective functions
- Definition of decision variables and constraints
- Data collection
- Generation and evaluation of alternatives
- Definition of selection criteria
- Selection of preferred alternatives
- Implementation of selected alternatives

The methodology began with the identification and quantification of objectives and the definition of decision variables and constraints—that is the optimization model formulation.

Critical analysis of approaches followed in the literature has uncovered the limitations of those based only on a single-objective model, which generally are based on an objective function (e.g., depth of cut, conicity, or cost per unit-machined length). The results of such a procedure give rise to a suboptimization, and generally, the results obtained for an optimization process based on different objective functions are in conflict.

To capture the complexity of the HAJM optimization problem, a multi-objective optimization model was developed based on suitable and conflicting objective functions that were selected to match the actual choices available to an industrial planner or decisionmaker. Therefore, an objective function has been selected from the first class in Table 2, as material removal rate or productivity objective function. A second objective function has been selected from the third class, as a machining economy objective function. The decision variables have been selected from the more frequent and significant variables.

The limits of these variables have been set taking into account the available machining resources, such as water supply pressure, machining feed rate, abrasive mass flow rate, focuser nozzle diameters, and abrasive particle densities and sizes. Constraint functions of the decision variables have been selected taking into account machining, quality, and power functions. A machining constraint function can be expressed as, "the kerf depth to be machined must be equal or greater than the required depth." A quality constraint function can be expressed as kerf conicity, or kerf width, or kerf surface roughness. These quality constraints are justified, because in the industrial process, the machining process must only satisfy product quality design specifications.

The quality constraint function is particularly important when net-shape machining or high accuracy machining are required. From the experiments performed, these features are possible with the HAJM process.

The last constraint function can be expressed as a power constraint function, which is directly proportional to water hydraulic pressure and flow rate. Due to the characteristics of the hydraulic servo-control, operating at a constant pressure up to a maximum and at a flow rate up to a maximum, depending on the frequency of the high-pressure reciprocating plunger intensifier, this constraint function can be simplified, because it is always satisfied in the operating range when water pressure and flow rate comply with pressure and flow rate variable limits.

Finally, because of the hydraulic constant-pressure servo-control, flow rate depends only on pressure and on the primary nozzle diameter. A further simplification can be adopted by considering this primary nozzle diameter as a parameter equal to a suitable value.

Using the results of the analysis of HAJM variables and models, HAJM optimization has therefore been studied as a multi-objective optimization problem,[8,34-41] where the following two objectives are defined: an economy function to be minimized and a productivity function to be maximized, whose variables have to comply with the resource limits and have to satisfy the machining, quality, and power constraint functions.[38] From the previous analysis on HAJM variables, a six-dimensional column vector, $\mathbf{x}$, of the decision variables used in the optimization model can be defined as follows:

$$\mathbf{x} = [x_i] \qquad i = 1,2,\ldots,6 \qquad [10]$$

where

$x_1 = P$ (water supply pressure)
$x_2 = u$ (feed rate)
$x_3 = \dot{m}$ (abrasive mass flow rate)
$x_4 = d_j$ (focuser diameter and jet diameter)
$x_5 = \rho_P$ (abrasive particle density)
$x_6 = G_r$ (abrasive particle size)

x_1, x_2, and x_3 are continuous, whereas x_4, x_5, and x_6 are discrete in practice.

With reference to the models, expressed in Eq 4 as a machining constraint function and in Eq 8 as a quality constraint function, the following quantities can be considered as parameters for the different classes:

- Material: σ, material dynamic flow stress; Cf, friction coefficient; V_c, threshold particle velocity
- Hydraulic power: $\bar{d}_n$ primary nozzle diameter (i.e., to satisfy the hydraulic power limit at the maximum pressure)
- Prediction: C_1, impact efficiency; K, conicity factor
- Machining conditions: $\bar{h}$, requested kerf depth; $\bar{\delta}$, requested kerf conicity
- Model limits: $\bar{s}$, standoff distance; $\bar{\alpha}$, cutting angle; $\bar{N}$, number of cutting passes

After evaluation of the $\mathbf{x}$ vector optimal conditions, other values of x_i optimizing variables can be evaluated, if needed, in terms of:

- Nozzle: ξ, mixing coefficient of the nozzle; d_n, primary nozzle diameter
- Abrasive: mP, abrasive particle mass; rP, abrasive particle radius; IP, abrasive particle moment of inertia
- Machining: N, number of cutting passes

The X space, or feasible solution region, can be defined in terms of constraints on the following variables:

$$X = \{\mathbf{x} \mid X_i,\ i = 1,2,\ldots,6;\ g_j \le 0,\ j = 1,2,3;\ \mathbf{x} \ge 0\} \qquad [11]$$

where

$$\begin{aligned}
X_1 &= \{x_1 \mid x_{1m} \le x_1 \le x_{1M}\} \\
X_2 &= \{x_2 \mid x_{2m} \le x_2 \le x_{2M}\} \\
X_3 &= \{x_3 \mid x_{3m} \le x_3 \le x_{3M}\} \\
X_4 &= \{x_{4k}\} \qquad k = 1,2,\ldots,m \\
X_5 &= \{x_{5l}\} \qquad l = 1,2,\ldots,n \\
X_6 &= \{x_{6r}\} \qquad r = 1,2,\ldots,p \\
g_1(x_i) &\le 0 \\
g_2(x_i) &\le 0 \\
g_3(x_i) &\le 0
\end{aligned} \qquad [12]$$

In the above, X_i ($i = 1,2,\ldots6$) subspaces and g_q ($q = 1,2,3$) constraint functions:

- x_{1m} and x_{1M} are, respectively, the feasible minimum and maximum pressure.
- x_{2m} and x_{2M} are, respectively, the feasible minimum and maximum feed rate.
- x_{3m} and x_{3M} are, respectively, the feasible minimum and maximum abrasive mass flow rate.
- x_{4k}, x_{5l}, and x_{6r} are, respectively, the available focuser nozzle diameters, abrasive particle densities, and abrasive particle sizes.

The constraint function $g_1(x_i)$ can be expressed as:

$$g_1(x_i) = \bar{h} - h(x_i) \qquad [13]$$

as the kerf depth constraint function, where $\bar{h}$ is the requested kerf depth, and $h(x_i)$ is the kerf depth predicted by the model expressed in Eq 4:

$$g_2(x_i) = \delta(x_i) - \bar{\delta} = [(D_0 - D_m(x_1, x_2, \bar{h})/\bar{h}] - \bar{\delta} \qquad [14]$$

as the kerf conicity constraint function, where $\bar{\delta}$ is the requested kerf conicity, and D_m can be evaluated by the model expressed in Eq 8.

The constraint function $g_3(x_i)$ generally can be expressed as a power constraint function that is directly proportional to water pressure and flow rate as:

$$g_3(x_i) = \beta\, x_1^{3/2}\, \bar{d}_n^2 - \bar{W} \qquad [15]$$

where $\bar{d}_n$ is the diameter of the primary nozzle; β is a coefficient proportional to nozzle efficiency; and W is the maximum available hydraulic power. In this case, because the hydraulic system has a constant-pressure servo-control and a limit on the frequency of the reciprocating plunger intensifier, i.e., a limit on water flow rate, Eq 15 and the last expression in Eq 12 are satisfied when x_1 pressure complies with the pressure constraint, expressed by the first expression in Eq 12 and the primary nozzle diameter, $\bar{d}_n$, satisfies the flow rate limit and the power limit at the maximum pressure.

This optimization model and HAJM process prediction and optimization module are not limited to these specific process models, but they can be adopted to any other physical or semi-empirical process model.

To define a multi-objective function, the following single-objective functions must be defined: $f_1(\mathbf{x})$, an economical single-objective function based on $C(x_i)$ direct cost per unit-machined length, or unit-removed volume per unit time, which must be minimized (see Table 2); $f_2(\mathbf{x})$, a productivity, or material-removal rate, single-objective function based on the $\dot{A}(x_i)$ removed area per unit time, which must be maximized (see Table 2).

The $f_1(\mathbf{x})$ objective function can be expressed as:

$$f_1(\mathbf{x}) = C(x_i) = \sum_j C_j(x_i) \quad j = 1,2,\ldots6 \qquad [16]$$

where $C_j(x_i)$ are the cost components of the economy function, respectively:

$$C_1(x_2, x_3) = c_a x_3/(\mu x_2) \qquad [16a]$$

is the specific cost of abrasive per machined unit length; where c_a is the abrasive cost per weight unit; μ is the abrasive effectiveness factor, or penalty factor, that takes into account abrasive particle hardness, shape, and breakdown, distribution and acceleration inside the focuser and at impingement:[42-44]

$$C_2(x_1, x_2) = c_{el}\eta\gamma\, x_1^{3/2}/x_2 \qquad [16b]$$

is the cost of the electrical power per machined unit length; where c_{el} is the electrical power variable cost; η is the global efficiency; $\gamma = (\pi/4)\bar{d}_n^2(2/\rho)^{1/2}$, where ρ is the water density, and $\bar{d}_n$ is the primary nozzle diameter:

$$C_3(x_1, x_2) = c_w\gamma\, x_1^{1/2}/x_2 \qquad [16c]$$

is water cost per machined unit length, where c_w is the water cost:

$$C_4(x_1, x_2, x_3) = \varepsilon x_1 x_3/x_2 \qquad [16d]$$

$$C_5(x_1, x_2) = \varphi x_1^{1/2}/x_2 \qquad [16e]$$

$$C_6(x_1, x_2) = \psi x_1^{3/2}/x_2 \qquad [16f]$$

are penalty cost functions, respectively, C_4 of the focuser nozzle, C_5 of the primary nozzle, C_6 of the intensifier, that take into

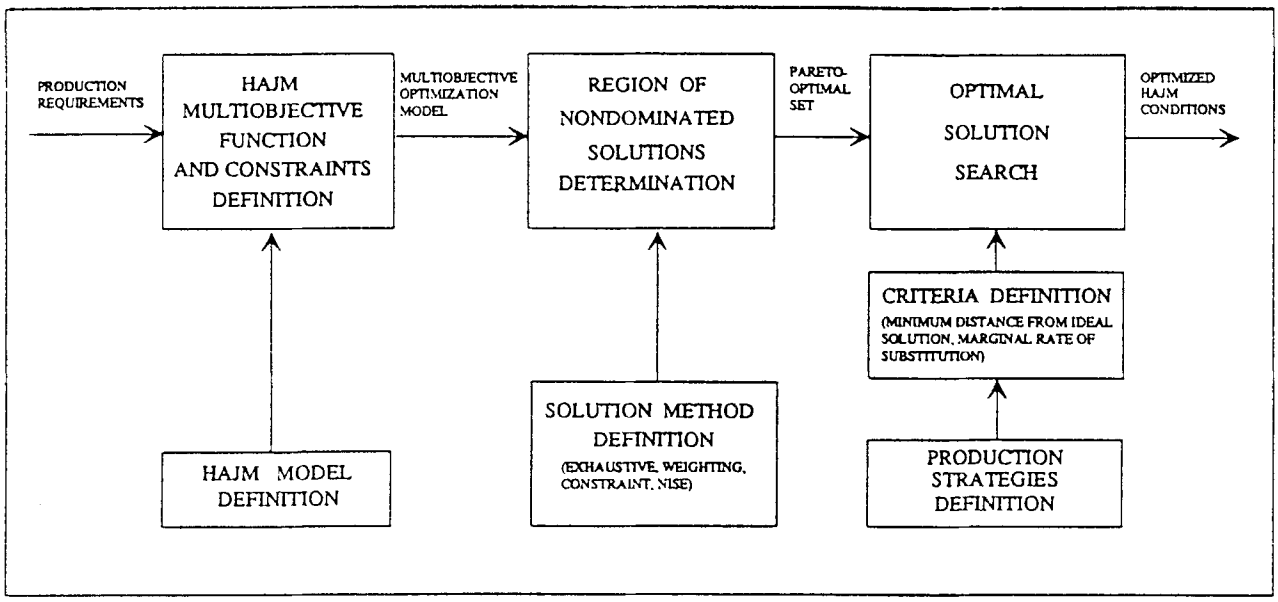

Fig. 4 HAJM multi-objective optimization model.

account the wear in these components. ε, φ, and ψ are penalty factors.

The $f_2(\mathbf{x})$ objective function can be expressed:

$$f_2(\mathbf{x}) = \dot{A}(x_i) = h(x_i)x_2 \qquad [17]$$

where $h(x_i)$ is the kerf depth predicted by the model expressed in Eq 4.

Then, the objective function $\mathbf{f}(\mathbf{x})$ can be defined for this multi-objective optimization problem as:

$$\mathbf{f}(\mathbf{x}) = [-f_1(x_i), f_2(x_i)] \qquad [18]$$

Therefore, the multi-objective optimization problem can be formulated:

$$\text{Maximize } \mathbf{f}(x_i) \text{ subject to } x_i \varepsilon X \qquad [19]$$

This multi-objective optimization problem can be solved following the planned methodology. The generation and evaluation of alternatives, definition of selection criteria, and selection of preferred alternatives can be performed after definition of the HAJM models, single-objective functions, multi-objective function, and set of constraints, as follows (see Fig. 4):

- Definition of solution methods
- Determination of the region of the nondominated solutions, or determination of F_{PO}, the Pareto-optimal set in the Y objective functions space, that contains the decision alternatives
- Definition of production strategies and searching criteria for the selection of the HAJM optimal solution

Techniques for generating nondominated or noninferior solutions of the formulated multi-objective optimization model, such as the weighting method, constraint method, noninferior set estimation (NISE) method,[34,37-39] have been studied for use in the HAJM process prediction optimization module. To directly analyze the Y space, F_{PO}, and the Pareto-optimal set, a program based on an extensive algorithm has been developed and implemented . The Y space has been determined by evaluating the (f_1, f_2) couple corresponding to the $[x_i]$ six-dimensional set of possible values. In the Y space, F_{PO} is then determined by making a graphical representation of the Y space. This noninferior set exhibits a "kinked" shape that justifies the use of generating methods as the weighting, constraint, or the NISE method. The optimum conditions are found in the vicinity of the "kink."

To determine the optimum solution, if no criterion or preference has been expressed for economy or productivity single-objective functions, the minimum distance from the ideal solution (or the utopia point) criteria can be used to:[34,38,45,46]

$$\begin{aligned} \text{minimize } d &= [(f_1 - f_1^*)^2 + (f_2 - f_2^*)^2]^{1/2} \\ &= [\Sigma_k (f_k(x_i) - f_k^*)^2]^{1/2} \quad k = 1,2 \\ \text{subject to } & (f_1, f_2) \varepsilon F_{PO} \end{aligned} \qquad [20]$$

where f^*, the coordinates of the ideal solution in the objective space, are the optima for each objective (f_1^*, f_2^*).

For this criteria, the optimized solution is the point of the pareto-optimal set at the minimum distance from the ideal solution of the Y space, corresponding to a minimum f_1 and maximum f_2, which is generally not feasible. When a specific production strategy is defined by the decisionmaker, the search

Table 3 Abrasive types and properties for HAJM optimization model test cases

Abrasive	Density, kg/dm^3	Abrasive particle size and roundness, mesh-adim.	Mohs hardness	Abrasive effectiveness factor (adim.)	Medium unit-cost, Lit/kg
<1> Glass grit	2.53	16 (1)-36 (1) 60 (1)-80 (1) 100 (1)	6.80	0.68	1500
<2> Silicon carbide	3.20	16 (0.31)-36 (0.31) 60 (0.31)-80 (0.31) 100 (0.31)	9.5-9.7	0.96	2000
<3> Olivine sand	3.30	36-60 80-100	6.5-6.7	0.66	400
<4> Natural garnet	3.9-4.1	16 (0.52)-36 (0.48) 60 (0.42)-80 (0.40) 100 (0.40)	8.0-9.0	0.85	1200
<5> Synthetic red corundum	4.00	16-36-60 80-100	9.00	0.90	1300
<6> Zirconia sand	4.6-4.8	36-60 80-100	6.5-7.0	0.67	1000

of the optimal solution can be obtained by defining a utility function of the two-objective optimization problem as:

$$U(fi_1, f_2) = \bar{u} \qquad [21]$$

which can be represented by indifference or isopreference curves and which indicates the degree to which the decision maker is willing to sacrifice one objective in order to obtain the second objective. This establishes a tradeoff between the objectives. The slope of the indifference curve can be expressed by the marginal rate of substitution (MRS):

$$\text{MRS}_{12} = df_2/df_1 \,|_{U(f_1,f_2)=U(\bar{f}_1,\bar{f}_2)} \qquad [22]$$

where $\bar{f}_1$ and $\bar{f}_2$ are fixed values of the two objectives, which must be specified in the Y space because the slope of the MRS constantly changes.

Taking into account the specific shape of the F_{PO} for HAJM multi-objective optimization, the utility function can be assumed in a linear form as:

$$U(f_1,f_2) = \alpha f_1 + (1 - \alpha) f_2 \qquad [23]$$

where $0 \le \alpha \le 1$ represents a coefficient that expresses the tradeoff between the two objective functions. From the analysis of F_{PO}, it can be verified that, when $\alpha = 1$, the utility function is equal to $-f_1$ objective function, i.e., the single objective is the economy function, such as direct cost per unit-machined length or per unit-removed volume per unit time. When $\alpha = 0$, the utility function is equal to f_2 objective function, i.e., the single objective is the productivity or material removal rate.

Indifference or isopreference curves can be expressed as follows:

$$f_2 = [\alpha / (\alpha - 1)] f_1 + \bar{u} \qquad [24]$$

In the HAJM process, a suitable choice of α, slope of a straight line, can satisfy a specific tradeoff situation, when quality, productivity, or economy functions must be satisfied.

3.3 *Application of HAJM Optimization Model*

Algorithms of the prediction and optimization model have been implemented, tested, and evaluated under several machining conditions. The evaluated data were compared with data reported in the literature and with data directly obtained from physical experiments. To this purpose, some numerical experiments were planned and designed. A set of suitable abrasives was selected (glass grit, silicon carbide, olivine sand, natural garnet, synthetic red corundum, zirconia sand). Their properties are listed in Table 3. The abrasive properties considered include:

- Density (ρp), which is a discrete variable in the cutting constraint function (Eq 13), based on the prediction model expressed by Eq 4
- Abrasive particle size (G_r), which is a discrete variable of the optimization model expressed by Eq 10
- Roundness factor (Rf), which is a variable in the selected prediction model corresponding to abrasive particle size
- Hardness, which is proportional to the abrasive effectiveness factor (μ), which has an effect on the specific cost of abrasive per machined unit-length (Eq 16a)
- Abrasive unit-cost (c_a), which is the abrasive cost per weight-unit (Eq 16a)

In these test cases, the abrasive effectiveness factor, μ is a linear function of hardness, but it can be considered as a penalty factor taking into account other attributes such as the shape and breakdown properties of abrasives.

From the results of the multi-objective optimization, the optimum combination of properties in terms of density, abrasive particle size, and hardness facilitate the selection of the optimal abrasive type.

The HAJM optimization tests were designed for three types of metals— an aluminum alloy (2024 T3), carbon steel (C30), and gray cast iron (G30). The parameters used in the three test cases are shown in Table 4; they are summarized as follows.

For the aluminum alloy in test 1, the material dynamic flow stress (σ) is replaced by $E/14$ (where E is the Young's modulus), which is the minimal predicted numerical deviation from the experimental results,[13] equal to 5210 MPa; V_c is equal to 40 m/s. For the carbon steel in test 2, σ = 14,800 MPa, V_c = 90 m/s. For the gray cast iron in Test 3, σ = 7860 MPa; V_c = 75 m/s. For all the three optimization tests, $\bar{h}$ = 100 mm; $\bar{\delta}$ = 0.5 mm; $\bar{d}_n$ = 0.25 mm.

Table 4 Range of the optimization test variables

Variables	Test 1	Test 2	Test 3
$X_1 = P$, bar	1500 min; 3500 max	1500 min; 3500 max	1500 min; 3500 max
$X_2 = u$, mm/min ...	5 min; 155 max	5 min; 155 max;	5 min; 155 max
$X_3 = m$, g/min.....	100 min: 1000 max	100 min; 1000 max	100 min; 1000 max
$X_4 = d_f$, mm.....	0.75-0.80-1.00	0.75-0.80-1.00	0.75-0.80-1.00
$X_5 = p$, kg/dm^3	2.53-3.2-3.3-3.9-4.0-4.7		
$X_6 = R_f$, mesh	30-50-80-120-150-220		

To determine the Y space of the **f** objective function, an extensive algorithm was implemented. In the test cases, suitable increments of the optimization model decision variables were used. Figures 5 to 7 show the graphical representation of the Y space, for the three test cases, which exhibited the anticipated "kinked" shape. For a suitable graphical representation of the Y space, the scales of the two axes were selected according to the different values assumed by f_1 and f_2 for the three test cases. On the horizontal axis, f_1, the economy objective function (cost per unit-length), is represented in Lit/m (Italian Lire/meter), whereas on the vertical axis, f_2, the productivity objective function (removed area per unit-time), is represented in mm^2/min.

Because some decision variables in the six-dimensional set are discrete and the optimization solution is discretized by the extensive algorithm, the density of the (f_1, f_2) points is not uniform. Analysis of the three different Y spaces indicates that the difference in density among the (f_1, f_2) points is due to the mechanical properties of the material (σ and V_c). When the material exhibits higher σ and V_c, fewer machining conditions satisfy the machining constraints.

In the F_{PO} region of the nondominated solutions, the pareto-optimal set can be determined; as shown in Fig. 5 to 7 (points A to P are for test 1; from A to H are for tests 2 and 3).

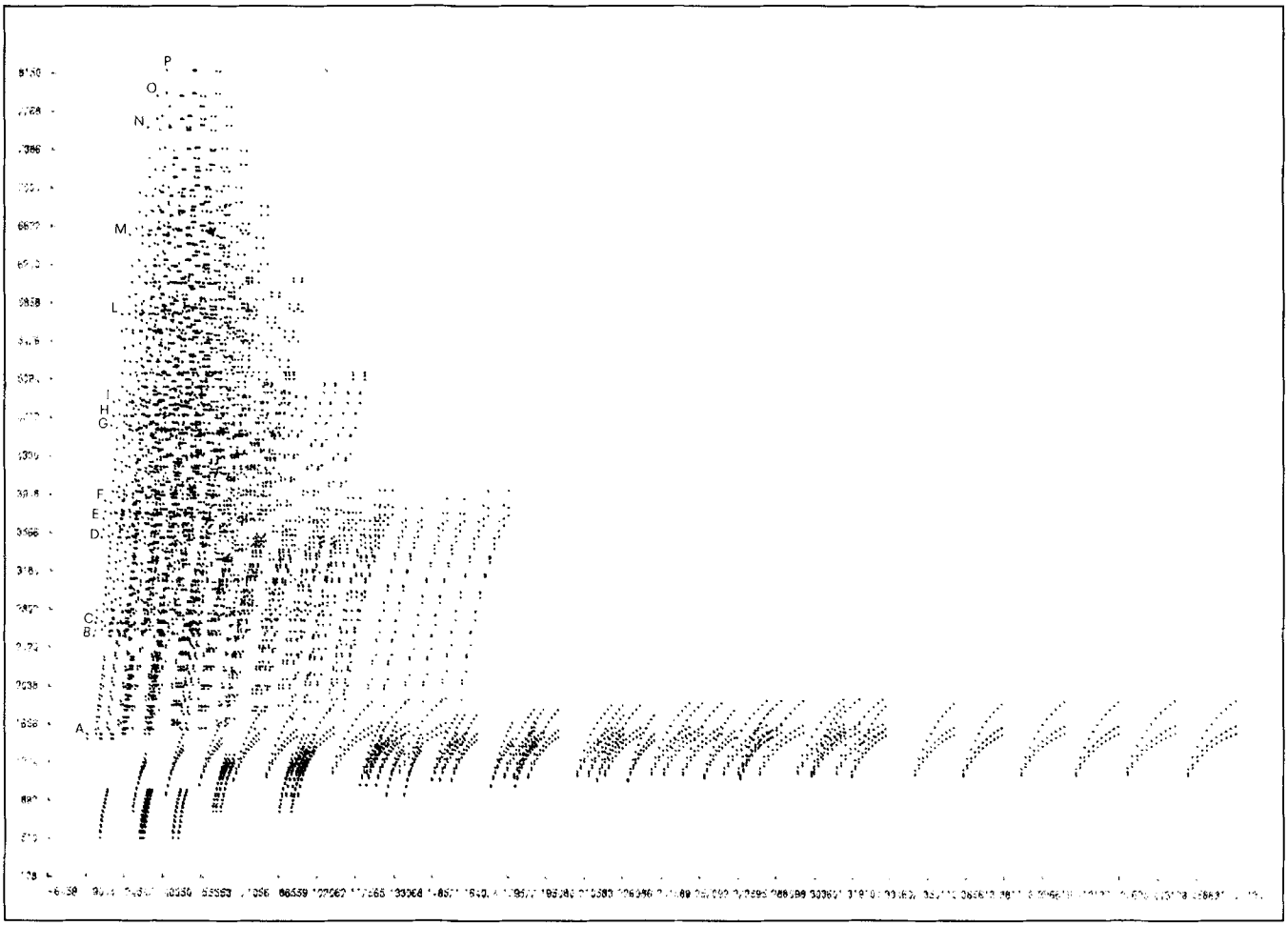

Fig. 5 Test 1: Graphical representation of Y space and F_{PO} of **f** objective function (horizontal axis: f_1[Lit/m]; vertical axis; f_2[mm^2/min]).

The nondominated solutions with the corresponding values of the six-dimensional variable set are given in Tables 5 to 7.

Note in the three test cases that $G_r(x_6)$ can assume any value from the selected range. The optimal abrasive is always the less expensive. The f_1 economy function is influenced primarily by the abrasive flow rate. Sensitivity analysis of the different variables shows that increases in water pressure, feed rate, and abrasive flow rate lead to corresponding increases in the f_1 and f_2 objective functions. A more complete sensitivity analysis is reported in Ref 8.

Table 5 Test 1: Nondominated solutions with corresponding values of the six-dimensional variable set

	$P(x_2)$, MPa	$u(x_2)$, mm/min	m (x_3), g/min	$d_j(x_4)$, mm	$\rho_P(x_5)_3$ kg/dm^3	$Gr(x_6)$, mesh	f_1, Lit/m	f_2, mm^2/min
A	350	15	100	0.80	3.30	...	9,044	1505.2
B	330	25	200	0.75	3.30	...	12,313	2659.1
C	350	25	200	0.75	3.30	...	12,774	2783.9
D	310	35	300	0.75	3.30	...	14,850	3512.9
E	330	35	300	0.75	3.30	...	15,480	3699.4
F	350	35	300	0.75	3.30	...	16,110	3879.4
G	330	45	400	0.75	3.30	...	18,513	4625.8
H	350	35	500	0.75	3.30	...	19,315	4860.5
I	310	45	500	0.75	3.30	...	21,753	4878.9
L	350	45	600	0.75	3.30	...	28,092	5824.6
M	350	55	700	0.80	3.30	...	30,748	6605.1
N	350	75	800	0.75	3.30	...	32,518	7606.9
O	350	75	900	0.75	3.30	...	36,368	7914.7
P	350	75	1000	0.75	3.30	...	40,217	8167.6

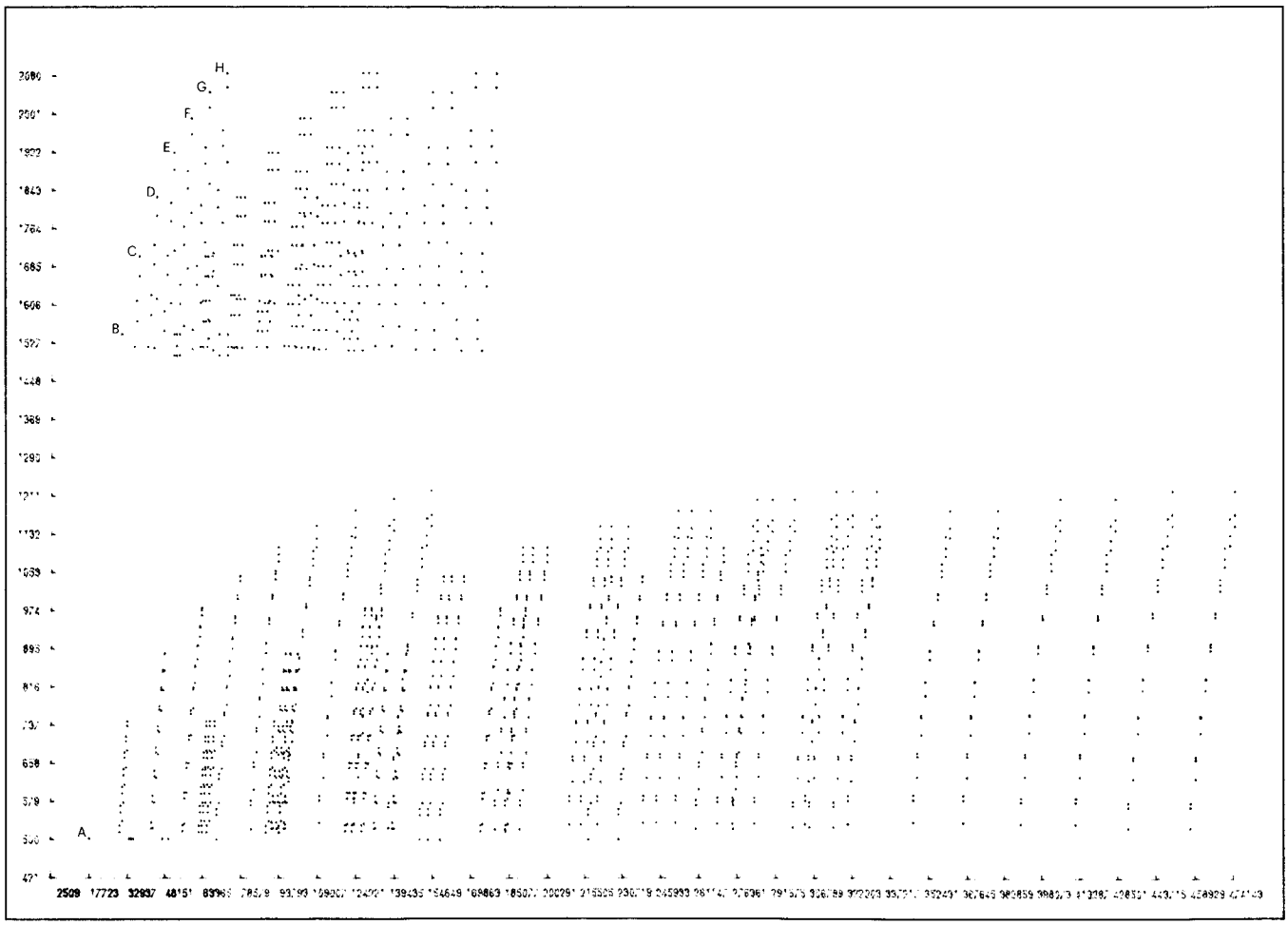

Fig. 6 Test 2: Graphical representation of Y space and F_{PO} of **f** objective function (horizontal axis: f_1[Lit/m]; vertical axis: f_2[mm^2/min]).

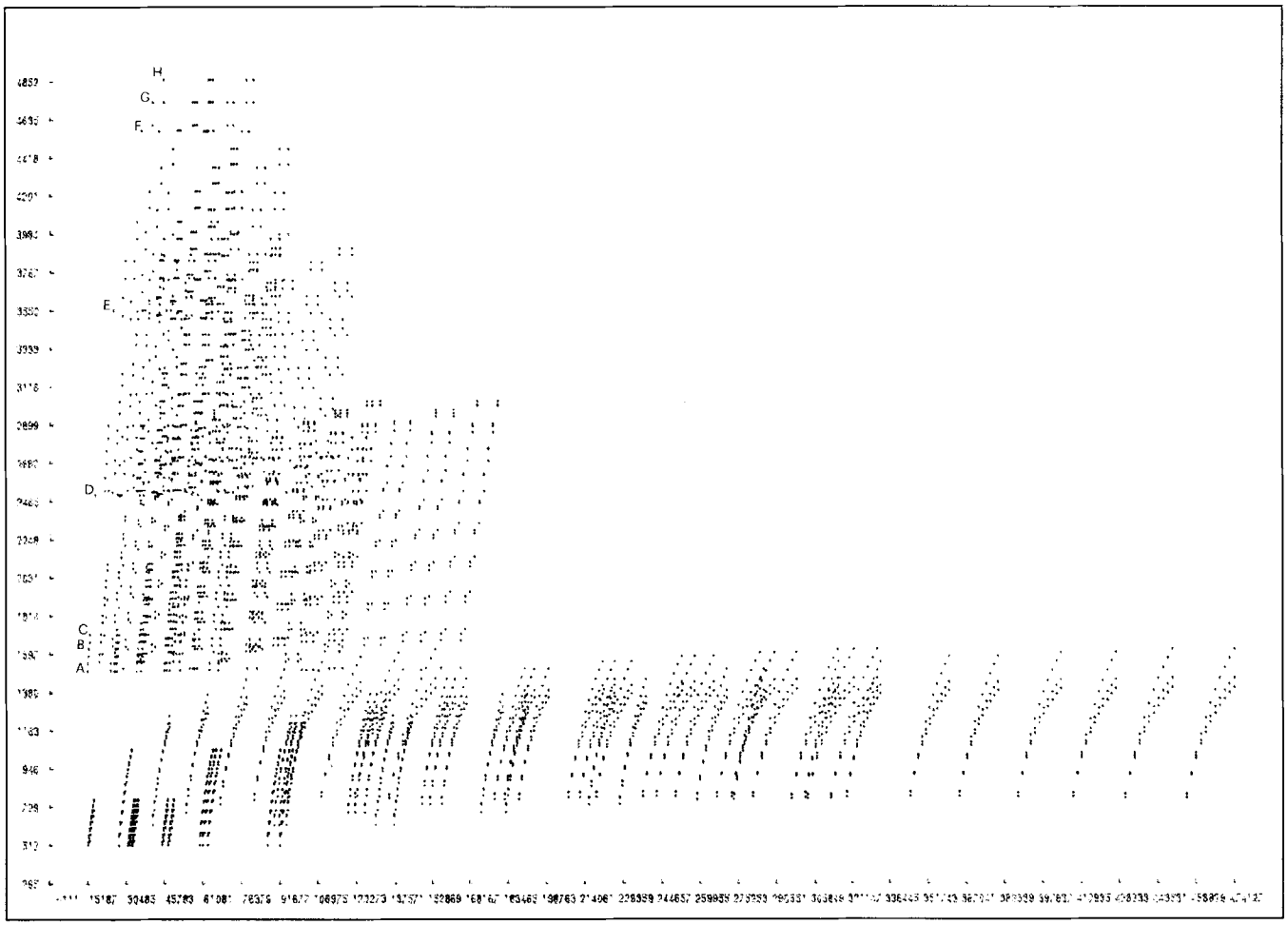

Fig. 7 Test 3: Graphical representation of Y space and F_{PO} of **f** objective function (horizontal axis: f_1[Lit/m]; vertical axis: f_2[mm^2/min]).

Table 6 Test 2: Nondominated solutions with corresponding values of the six-dimensional variable set

	P (x_2), MPa	u (x_2), mm/min	m (x_3), g/min	d_j (x_4), mm	ρ_P (x_5), kg/dm^3	Gr (x_6), mesh	f_1, Lit/m	f_2, mm^2/min
A	350	5	100	0.75	3.30	...	17,723	502.2
B	350	15	400	0.75	3.30	...	30,289	1546.0
C	350	15	500	0.75	3.30	...	37,371	1707.2
D	350	15	600	0.75	3.30	...	44,453	1829.2
E	330	15	700	0.75	3.30	...	51,534	1922.2
F	350	15	800	0.75	3.30	...	58,616	1993.0
G	350	15	900	0.75	3.30	...	65,698	2046.6
H	350	15	1000	0.75	3.30	...	72,780	2086.3

To evaluate the optimal solution, if the minimum distance from the ideal solution, or utopia point criterion is adopted, from test 1 (Fig. 5, Table 5) the optimal point is B, from test 2 (Fig. 6, Table 6) the optimal point is A, from test 3 (Fig. 7, Table 7), the optimal point is B. These optimal points correspond to high pressure, low feed rate, and low abrasive mass flow rate. Among the six-dimensional set of optimal solution variables, feed rate and abrasive mass flow rate depend on the workpiece material characteristics.

On the contrary, however, if the MRS criterion is adopted (considering a linear form for the utility function as expressed by Eq 23), for test 1, when $\alpha = 0$, the objective function corresponds to the productivity objective function and the optimal point is P. When $\alpha = 1$, the objective function corresponds to the economy objective function, and the optimal point is A.

Due to the kinked, flat shape of the F_{PO} region, a sensitivity analysis of the α coefficient demonstrates that for test 1 increments to α, from $\alpha = 0$ and in the proximity of $\alpha = 0$, lead to

Table 7 Test 3: Nondominated solutions with corresponding values of the six-dimensional variable set

	$P(x_2)$, MPa	$u(x_2)$, mm/min	$m(x_3)$, g/min	$d_j(x_4)$, mm	$\rho_P(x_5)_3$ kg/dm^3	$Gr(x_6)$, mesh	f_1, Lit/m	f_2, mm^2/min
A	310	15	200	0.75	3.30	...	15,187	1548.0
B	330	15	200	0.75	3.30	...	15,656	1631.2
C	330	15	200	0.75	3.30	...	16,126	1711.3
D	350	25	300	0.75	3.30	...	18,239	2502.2
E	350	35	500	0.75	3.30	...	26,656	3554.2
F	350	45	80	0.75	3.30	...	36,868	4575.8
G	350	45	900	0.75	3.30	...	41,256	4736.7
H	350	45	1000	0.75	3.30	...	45,644	4863.2

different optimal solutions (from point B to point P), and that for the other values of α up to 1, the optimal solution coincides with point A. This means that if the productivity objective function is preferred by the decisionmaker, the resultant optimal solution varies, whereas if the economy objective function is preferred, the optimal solution coincides with the optimal solution that results when the multi-objective function is equal to the single economy objective function.

4. Conclusions

This article has presented the approach followed for HAJM computer control and optimization and for the implementation, automation, and integration of a HAJM cell. A hierarchical control architecture has been presented. Suitable HAJM prediction models have been analyzed. A multi-objective optimization model has been defined and implemented in a process prediction and optimization module that was integrated into the control architecture. In addition to providing optimized HAJM conditions for economy and productivity optimization and satisfying the constraints of required kerfing depth and cutting quality and available machining resources, this module has established a basis for the further use of adaptive control constraint (ACC), adaptive control optimization (ACO), and CAD/CAM integration.

Acknowledgments

This work was carried out with funding of the Italian MURST (Ministry of University and Scientific and Technological Research) and CNR (National Research Council). The authors are grateful to UHDE GmbH—Werk Hagen (Germany), SOITAAB s.a.s.—Ronco Briantino, Milano (Italy), OSAI A-B S.p.A.—Ivrea, Torino (Italy) for their support. The experimental facilities were partially supplied within commodatum contracts between Politecnico di Milano—Dipartimento di Meccanica and UHDE GmbH, and SOITAAB s.a.s. The authors are also grateful to their student Giuseppe Comi, who cooperated to the development and implementation.

References

1. L.R.K. Gillespie, *Deburring Technology for Improved Manufacturing*, Society of Mechanical Engineers, 1981, p 437-447
2. M. Hashish, "Milling with Abrasive-Waterjets: A Preliminary Investigation," Proc. 4th U.S. Waterjet Conference, BHRA, 1987, p 1-10
3. M. Hashish, Turning with Abrasive-Waterjets—A First Investigation, *Trans. ASME J. Eng. Ind.*, Vol 111, 1987, p 158-166
4. M. Hashish, "Turning, Milling, and Drilling with Abrasive-Waterjets," Proc. 9th Int. Symp. Jet Cutting Technol., BHRA, Sendai, 1988, p 113-131
5. M. Hashish, An Investigation of Milling with Abrasive-Water Jets, *Trans. ASME J. Eng. Ind.*, Vol 111, 1989, p 158-166
6. H. Blickwedel, N.S. Guo, H.e.H. Louis Haferkamp, "Prediction of Abrasive Jet Cutting Efficiency and Quality," Proc. 10th. Int. Symp. Jet Cutting Technology, BHRA, Amsterdam, 1990
7. K. Faber and H. Oweinah, "Influence of Process Parameters on Blasting Performance with Abrasive-Jet," Proc. 10th Int Symp. Jet Cutting Technol., Amsterdam, 1990
8. R. Groppetti and G. Comi, "Contribution to Computer Control and Optimization of Hydro-Abrasive Jet Machining Process," Proc. 1991 ASME Int. Computers in Engineering, Santa Clara, 1991
9. M. Hashish, "The Application of Abrasive Jets to Concrete Cutting," Proc. 6th Int. Symp. Jet Cutting Technol., BHRA, Guildford, 1982, p 447-464
10. M. Hashish, "Steel Cutting with Abrasive Waterjets," Proc. 6th Int. Symp. Jet Cutting Technol., BHRA, Guildford, 1982, p 465-488
11. R.K. Miller, *Water Jet Cutting, Technology and Industrial Application*, The Fairmont Press, Lilburn, 1991, p 3-19/26-42/72-88
12. S. Yanagiuchi and H. Yamagata, Cutting and Drilling of Glass by Abrasive Jet, Proc. 8th Int. Symp. Jet Cutting Technol., BHRA, Durham, 1986, p 323-330
13. M. Hashish, A Model for Abrasive-Waterjet (AWJ) Machining, *Trans. ASME J. Eng. Mater. Technol.*, Vol 111, 1989, p 154-162
14. W. König and Ch. Wulf, "The Influence of the Cutting Parameters on Jet Forces and the Geometry of the Kerf," Proc. 7th Int. Symp. Jet Cutting Technol., BHRA, Ottawa, 1984, p 179-192
15. M. Mazurkiewicz and P. Karlic, "Material Dynamic Response during Hydroabrasive Jet Machining (HAJM)," Proc. 4th U.S. Water Jet Conference, ASME, Berkeley, 1987, p 159-167
16. R. Groppetti, "Implementing CIM in an Experimental Environment Methodology and Case Study," Proc. 27th Int. Machine Tools Design and Research Conf., UMIST, Manchester, 1988
17. C. Borasio, R. Groppetti, P. Murchio, and D. Sola, "Experimental Center for System Integration in CIM," ESPRIT Conference, Brussels, North Holland, 1987
18. R. Groppetti, "On the Development of a CIM Experimental Center," Proc. 17th ISATA, Munich, 1987
19. R. Groppetti and G. Comi, Studio di una Cella per Processo HAJM (Hydro-Abrasive Jet Machining): Analisi e Sintesi del Sistema di Controllo, Rapporto di Ricerca RG-03-90, Dipartimento di Meccanica, Politecnico di Milano, 1990
20. R. Groppetti and G. Comi, Studio ed Implementazione di Algoritmi di Predizione dello Spessore Tagliato Mediante HJM (Hydro-Jet Machining) e HAJM (Hydro-Abrasive Jet Machining), Rapporto di Ricerca RG-04-90, Dipartimento di Meccanica, Politecnico di Milano, 1990

21. H.-J. Jacobs, B. Hentschel, and B. Stange, Intelligent Tool Monitoring for Machining, *Int. J. Prod. Res.*, Vol 26, 1988, p 1579-1592
22. R. Groppetti and G. Comi, Analisi Critica di Alcuni Modelli del Processo HAJM (Hydro-Abrasive Jet Machining), Rapporto di Ricerca RG-02-90, Dipartimento di Meccanica, Politecnico di Milano, 1990
23. M. Hashish, Pressure Effects in Abrasive-Waterjet (AWJ) Machining, *Trans. ASME J. Eng. Mater. Technol.*, Vol 111, 1989, p 221-228
24. M. Hashish and M.P. Du Plessis, Theoretical and Experimental of Continuous Jet Penetration of Solids, *Trans. ASME J. Eng. Ind.*, Vol 100, 1978, p 88-94
25. M. Hashish and M.P. Du Plessis, Prediction Equations: High Velocity Jet Cutting Performance to Standoff Distance and Multipasses, *J. Eng. Ind.*, Vol 101, 1979, p 311-318
26. S. Kaliszky, *Plasticity—Theory and Engineering Applications*, Elsevier, Amsterdam, 1989
27. M. Hashish, A Modeling Study of Metal Cutting with Abrasive Waterjets, *Trans. ASME*, Vol 106, 1984, p 88-100
28. M. Hashish, Cutting with Abrasive Waterjets, *Mech. Eng.*, 1984, p 60-69
29. M. Hashish, "An Improved Model for Erosion by Solid Particle Impact," Proc. 7th Int. Conf. Erosion by Liquid and Solid Impact, ELSI VII, Cambridge, 1987
30. D.K.M. Tan, A Model for the Surface Finish in Abrasive-Waterjet Cutting, Proc. 8th Int. Symp. Jet Cutting Technol., BHRA, 1986, p 309-313
31. S. Yazici and D.A. Summers, "The Use of High Pressure Waterjets in Cutting Foam," Proc. 4th U.S. Water Jet Symp., BHRA, 1988, p 11-18
32. M. Hashish, Prediction on Depth of Cut in Abrasive-Waterjet (AWJ) Machining, *Trans. ASME J. Eng. Mater. Technol.*, 1988, p 65-82
33. H. Arasawa, K. Matsumoto, S. Yamaguchi, and K. Sumita, "Controlled Cutting of Concrete Structure with Abrasive Water-Jet," Proc. 8th Int. Symp. Jet Cutting Technol., BHRA, 1986, p 211-218
34. J.L. Cohon, Multiobjective Programming and Planning, *Mathematics in Science and Engineering*, Academic Press, 1978
35. A.M. Abuelnaga and M.A. Dardiry, Optimization Methods for Metal Cutting, *Int. J. Mach. Tool Des. Res.*, Vol 24, 1984, p 11-18
36. C.S. Beighter, D.T. Phillips, and D.J. Wilde, *Foundations of Optimization*, Prentice-Hall, 1973
37. B.S. Gottfried and J. Weisman, *Introduction to Optimization Theory*, Prentice-Hall, 1973
38. R. Groppetti and G. Comi, Studio ed Implementazione di un Algoritmo di Ottimizzazione Mediante Programmazione Multiobiettvi per il Processo HAJM (Hydro-Abrasive Jet Machining), Rapporto di Ricerca RG-05-90, Dipartimento di Meccanica, Politecnico di Milano, 1990
39. C. Hwang and A.S. Masud, *Multiple Objective Decision Making—Methods and Applications*, Springer-Verlag, 1979, p 164
40. R.L. Keeney and H. Raiffa, *Decisions with Multiple Objectives: Preferences and Value Tradeoffs*, John Wiley & Sons, 1976
41. M. Zeleny, *Multiple Criteria Decision Making*, Springer-Verlag, 1976, p 123
42. L. Coes, *Abrasives, Applied Mineralogy*, Vol 1, Springer-Verlag, 1971, p 24-28/141-153
43. T. Isob, H. Yashida, and K. Nishi, "Distribution of Abrasive Particles in Abrasive Water Jet and Accelerations Mechanisms," Proc. 9th Int. Symp. Jet Cutting Technol., Ottawa, 1984, p 179-192
44. M. Simpson, Abrasive Particle Study in High Pressure Water Jet Cutting, *Int. J. Water Jet Technol.*, Vol 1, 1990, p 17-28
45. P. Yu, A Class of Decisions for Group Decision Problems, *Manage. Sci.*, Vol 19, 1973, p 936
46. M. Zeleny, *Linear Multiobjective Programming*, Springer-Verlag, 1974